International Immunology, Vol. 26, No. 10, pp. 551–561
doi:10.1093/intimm/dxu057
Advance Access publication 22 May 2014

Generation of induced pluripotent stem cell-derived mice by reprogramming of a mature NKT cell

Yue Ren[1,2], Nyambayar Dashtsoodol[1], Hiroshi Watarai[1,3], Haruhiko Koseki[4], Chengshi Quan[2] and **Masaru Taniguchi[1]**

[1]Laboratory for Immune Regulation, RCAI, RIKEN Center for Integrative Medical Sciences (IMS-RCAI), 230-0045 Kanagawa, Japan
[2]The Key Laboratory of Pathobiology, Ministry of Education, Jilin University, Changchun, 130021 Jilin, People's Republic of China
[3]Precursory Research for Embryonic Science and Technology (PRESTO), Japan Science and Technology Agency (JST), 102-0076 Tokyo, Japan
[4]Laboratory for Developmental Genetics, RCAI, RIKEN Center for Integrative Medical Sciences (IMS-RCAI), 230-0045 Kanagawa, Japan

Correspondence to: M. Taniguchi; E-mail: taniguti@rcai.riken.jp

Received 9 March 2014, *accepted* 15 May 2014

Abstract

NKT cells are characterized by their expression of an NKT-cell-specific invariant antigen-receptor α chain encoded by Vα14Jα18 gene segments. These NKT cells bridge the innate and acquired immune systems to mediate effective and augmented responses; however, the limited number of NKT cells *in vivo* hampers their analysis. Here, two lines of induced pluripotent stem cell-derived mice (NKT-iPSC-derived mice) were generated by reprogramming of mature NKT cells, where one harbors both rearranged Vα14Jα18 and Vβ7 genes and the other carries rearranged Vα14Jα18 on both alleles but germline Vβ loci. The analysis of NKT-iPSC-derived mice showed a significant increase in NKT cell numbers with relatively normal frequencies of functional subsets, but significantly enhanced in some cases, and acquired functional NKT cell maturation in peripheral lymphoid organs. NKT-iPSC-derived mice also showed normal development of other immune cells except for the absence of γδT cells and disturbed development of conventional CD4 αβT cells. These results suggest that the NKT-iPSC-derived mice are a better model for NKT cell development and function study rather than transgenic mouse models reported previously and also that the presence of a pre-rearranged Vα14Jα18 in the natural chromosomal context favors the developmental fate of NKT cells.

Keywords: iPSC, NKT cell, TCR rearrangement

Introduction

NKT cells are characterized by their expression of an invariant TCR, Vα14Jα18 paired with Vβ8.2, Vβ7 or Vβ2 in mice and Vα24Jα18/Vβ11 in humans. These stereotypic TCRs recognize glycolipid antigens such as α-galactosylceramide (α-GalCer) in conjunction with the monomorphic MHC class I-like molecule, CD1d (1, 2). Recent studies have demonstrated that NKT cells can be classified into three different functional subtypes, IL-4/IL-13-producing, IL-17A-producing and IFN-γ-producing NKT cells, even though they all express the same invariant antigen receptor (3). These NKT cell subtypes mediate bystander immune regulatory functions, activating various immune effector cell types, including NK cells, macrophages, granulocytes, dendritic cells (DCs), basophils and eosinophils in the innate system as well as CD4 T and CD8 T cells in the acquired system. Therefore, NKT cells participate in the regulation of various disease states, including infection, autoimmunity, allergy, antitumor responses as well as maintenance of transplantation tolerance (1, 2). In fact, X-linked lymphoproliferative disease patients who lack NKT cells die from uncontrolled Epstein–Barr virus infection (4), and NKT-deficient mice also show a shorter survival time when infected with *Streptococcus pneumoniae* (5). Thus, NKT cells are essential to achieve effective immune responses. On the basis of these multiple functions, NKT cells are considered a promising target for immunotherapy, although there are still some limitations preventing the broad application of NKT cells, especially their extremely low frequency. To overcome this problem, the induced pluripotent stem cell (iPSC) technology is potentially a very powerful tool for analysis and application of NKT cells.

Another important issue in NKT cell biology is to understand the molecular mechanisms of their fate determination. In previous studies, rearranged Vα14Jα18 and Vβ8.2 genes were introduced into RAG-knockout (KO) mice and there was preferential generation of NKT cells but no NK cells, B cells or conventional T cells (6). Moreover, iPS cell lines obtained by reprogramming of mature NKT cells preferentially generate NKT cells but no αβT, γδT cells, NK cells, DCs or B cells *in vitro* (7). These results suggest that the pre-rearranged Vα14Jα18/Vβ8.2 TCR genes determine the NKT cell fate. On the other hand, Serwold *et al*. (8) have demonstrated abnormal T-cell development in the thymus of mice generated by nuclear transfer from mature conventional T cells. Thus, it is of interest to determine whether TCRα or TCRβ chain gene rearrangements are involved in cell fate determination *in vivo*, particularly in NKT cells.

Here, we successfully generated NKT-iPSC-derived mice by using an NKT cell-derived iPSC (NKT-iPSC) line that was reprogrammed from mature NKT cells of a wild-type (WT) C57BL/6 (B6) mouse. Two types of NKT-iPSC-derived mice are generated from this NKT-iPSC line: one carries a rearranged Vα14Jα18 on both alleles with the TCR Vβ loci in germline configuration (Vα14/WTVβ mice) and the other harbors rearrangements of both Vα14Jα18 and Vβ7 on both chromosomes (Vα14/Vβ7 mice). Both types of NKT-iPSC-derived mice had an increased number of NKT cells with relatively normal frequencies of the functional subsets, as well as normal development of all other cell types except for the absence of γδT cells and disturbed development of conventional CD4 αβT cells. Although NKT cells in Vα14/Vβ7 mice had immature phenotypes in the thymus, they acquired functional maturation in the peripheral lymphoid organs.

Methods

Generation of NKT-iPS-derived mice

Two lines of NKT-iPSC-derived mice (Vα14/WTVβ and Vα14/Vβ7) were generated as described in Results and Supplementary Figure 1, available at *International Immunology* Online. In brief, the NKT-iPSC line, designated iPSC-58 3E7, was established by reprogramming of mature splenic NKT cells from B6 mice with the Yamanaka factors (9) as previously described (7). The NKT-iPSCs were injected into BALB/c blastocysts to produce chimeric mice. After mating chimeras with B6 mice and genotyping their offspring, pups that harbored rearranged Vα14Jα18 and/or Vβ7 genes in their genomes were chose for further breeding to generate the NKT-iPSC-derived mice. Germline transmission of the rearranged Vα14Jα18 and Vβ7 loci was achieved with two male chimeras, designated as iPSC-58 3E7-1 and iPSC-58 3E7-2. Genotyping PCR primer sequences are listed in Supplementary Table S1, available at *International Immunology* Online.

Mice

B6 mice were purchased from Charles River Laboratories or CLEA Japan, Inc. Two lines of NKT-iPSC-derived mice (Vα14/WTVβ mice and Vα14/Vβ7 mice) and all other mice were kept under specific pathogen-free conditions and were used at 8–16 weeks of age unless otherwise indicated. All procedures were conducted according to protocols approved by the RIKEN Animal Care and Use Committee.

Flow cytometry

Antibodies (BD Biosciences, eBioscience and BioLegend) used were: APC-Cy7 and Brilliant Violet 421 anti-TCRβ (H57-597), FITC and Pacific Blue anti-CD4 (RM4-5), PE-Cy7 and FITC anti-CD8a (53–6.7), PE anti-CD8b.2 (53–5.8), PE-Cy7 anti-NK1.1 (PK136), PerCP-Cy5.5 anti-CD25 (PC61), FITC anti-CD25 (7D4), FITC anti-Vβ8.1/8.2 (MR5-2), FITC anti-Vβ7 (TR310), FITC anti-Vβ2 (B20.6), PE anti-TCRγδ (GL3), APC anti-TCRγδ (eBioGL3), APC anti-CD11c (HL3), FITC anti-CD19 (eBio1D3), PerCP-Cy5.5 anti-B220 (RA3-6B2), FITC and PE anti-CD3ε (145-2C11), PE anti-CD1d (1B1), PE anti-Ly108 (330-AJ), PE anti-CD150 (9D1), Pacific Blue anti-CD62L (MFL-14), FITC anti-CD24 (M1/69), PE anti-rat IgG1 (A110-1) and APC-eFluor 780 anti-CD117 (2B8). PE anti-FOXP3 (FJK-16s) was used for intracellular staining with BD Cytofix/Cytoperm™ Fixation/Permeabilization Kit (BD Biosciences) according to the manufacturer's directions. Biotinylated anti-mouse IL-17RB (B5F6) was prepared as previously described (10) and detected by staining with PE-Avidin. α-GalCer-loaded CD1d (α-GalCer/CD1d) dimer (BD Biosciences) for NKT cell enrichment and detection was prepared by the method described previously (11). Cells were analyzed with FACSCanto II (BD Biosciences) or FACSAria II (BD Biosciences). Cell sorting was done using FACSAria II (BD Biosciences). Data were analyzed by FlowJo software (Tree Star).

Quantitative real-time PCR and reverse transcription–PCR

RNA was isolated from FACS-sorted cells using the RNeasy Micro Kit (Qiagen), and cDNAs were generated with the High capacity cDNA Reverse Transcription Kit with RNAse Inhibitor (Applied Biosystems) according to the manufacturer's instructions. Quantitative real-time PCR (qPCR) primers and probes were designed with Universal Probe Library Assay (Roche) or TaqMan® Gene Expression Assay (Applied Biosystems). The primer sequences and probes are listed in Supplementary Table S2, available at *International Immunology* Online. qPCR was performed using the ABI PRISM 7900HT system (Applied Biosystems) with FastStart Universal Probe Master (Roche) or by LightCycler 480 (Roche Applied Science) with LightCycler 480 Probes Master (Roche). Results were analyzed using the ΔC_t method with *Gapdh* as the internal control with the Universal ProbeLibrary Mouse GAPD Gene Assay (Roche Applied Science). Reverse transcription–PCR (RT–PCR) was done with primers listed in Supplementary Table S3, available at *International Immunology* Online, using Ex Taq (Takara). PCR consisted of initial denaturation at 96°C for 3 min, followed by 28 cycles of amplification for *Gapdh* and 35 cycles for *Vα-Cα* variants with the thermal cycler conditions: 96°C for 30 s, 55°C for 20 s and 72°C for 1 min, and final extension at 72°C for 5 min. PCR products were stained with SYBR Safe DNA gel stain (Molecular Probes) and visualized with LAS-4000 image analyzer (Fuji Film, Japan).

Intracellular cytokine staining

FACS-sorted NKT cells (5×10^5) were stimulated with Cell Stimulation Cocktail (plus protein transport inhibitors; eBioscience) for 4 h, followed by intracellular cytokine staining using BD Cytofix/Cytoperm™ Fixation/Permeabilization Kit (BD Biosciences) according to the manufacturer's instructions. Antibodies (BD Biosciences or eBioscience) used for intracellular cytokine staining were FITC anti-IFN-γ (XMG1.2), PE anti-IL-4 (11B11) and eFluor 450 anti-IL-17A (eBio17B7). Cells were analyzed by FACSCanto II (BD Biosciences). Data were analyzed by FlowJo software (Tree Star).

Isolation of intraepithelial lymphocytes

After Peyer's patches and connective tissues were removed from small intestines, they were opened longitudinally, washed three times in ice-cold PBS buffer to clean their contents, then cut into 0.5 cm pieces and incubated with gentle stirring for 30 min at 37°C in RPMI 1640 containing 1% FCS (Gibco) and 1 mM EDTA. After incubation, tubes were shaken vigorously and the content was passaged through a 100 μm cell strainer (BD Falcon), centrifuged at 400 × *g* for 5 min and washed with PBS buffer containing 2% FCS. Then cell pellets were resuspended in 5 ml of 40% Percoll, and centrifuged at 2000 × *g* for 10 min. The resulting cell pellet was washed two times with PBS containing 2% FCS and used for flow cytometry analysis.

Statistical analysis

Data were presented as mean ± SD or mean ± SEM from three independent experiments. The statistical significance of differences was determined by the Student's *t*-test. Any difference with a *P* value of <0.01 was considered significant (*$P < 0.01$).

Results

Generation of NKT-iPSC-derived mice

We succeeded in reprogramming B6 mature splenic NKT cells with the Yamanaka factors (9) and established an NKT-iPSC line, designated iPSC-58 3E7. As already demonstrated in previous *in vitro* studies (7), the NKT-iPSCs preferentially generated α-GalCer/CD1d dimer$^+$ TCRβ$^+$ NKT cells but no αβT, γδT, DC, NK or B cells when co-cultured on either OP9 or OP9/Dll1 for 25 days in the presence of Flt3 ligand (Flt3L) and IL-7.

By using this NKT-iPSC line, germline transmission of the rearranged Vα14Jα18 and Vβ7 loci was achieved with two male chimeras, designated as iPSC-58 3E7-1 and iPSC-58 3E7-2 (Supplementary Figure 1A, available at *International Immunology* Online). Pups with rearranged Vα14Jα18 and/or Vβ7 (Supplementary Figure 1B, available at *International Immunology* Online) were further bred with B6 mice to generate two lines of NKT-iPSC-derived mice harboring Vα14Jα18 on both alleles with germline TCRVβ (Vα14/WTVβ mice) or Vα14Jα18 and Vβ7-Dβ2-Jβ2.3 on both respective alleles (Vα14/Vβ7 mice). These mice were used for the present study.

Preferential development of NKT cells in Vα14/WTVβ and Vα14/Vβ7 mice

Both Vα14/WTVβ and Vα14/Vβ7 mice showed increased numbers and percentages of α-GalCer/CD1d$^+$ NKT cells in the thymus, spleen and liver compared to B6 mice (Fig. 1A and B). In B6 mice, the absolute number of NKT cells was 4.5×10^5 in the thymus, 5.7×10^5 in the spleen and 2.9×10^5 in the liver. By contrast, there was a threefold increase in NKT cell numbers in the thymus of Vα14/WTVβ (14.7×10^5) and Vα14/Vβ7 (15.1×10^5) mice, while NKT cells in the spleen (91×10^5 in Vα14/WTVβ, 133×10^5 in Vα14/Vβ7 mice) and liver (21×10^5 in Vα14/WTVβ, 44×10^5 in Vα14/Vβ7 mice) were about 10- to 20-fold higher than in B6 mice (Fig. 1B). Under physiological conditions, NKT cells have a strong bias for Vβ8, Vβ7 and Vβ2 usage due to the positive selection mediated by CD1d (12). A similar bias was seen in the Vβ repertoire of NKT cells from Vα14/WTVβ mice (Fig. 1C). On the other hand, the NKT cells in Vα14/Vβ7 mice were monoclonal and all cells exclusively used Vβ7 due to allelic exclusion by the Vβ chain gene locus (13). These results suggest that a normal selection process is taking place during NKT cell development in the thymus. In fact, genes and molecules important for NKT cell development, including CD1d (7, 11) and SLAM family receptor Ly108 (14) (encoded by *Slamf6*), *SAP* (4, 15, 16), *Fyn* (17, 18), *c-Myb* (19), *c-Myc* (20, 21), *Runx1* (22), *HEB* (23) and *Egr2* (24), were expressed at normal levels in the thymic CD4/CD8 double-positive (DP) populations in NKT-iPSC-derived mice (Fig. 1D and E), where positive selection of NKT cells is believed to take place (25).

Collectively, the rearranged Vα14 gene directs robust differentiation towards the NKT cell lineage, and there is preferential development of NKT cells in mice generated from NKT-iPSC.

Lymphocyte development in Vα14/WTVβ and Vα14/Vβ7 mice

We also investigated development of other thymocyte subsets in the NKT-iPSC mice. The absolute number of total thymocytes was severely decreased in both Vα14/WTVβ and Vα14/Vβ7 mice, indicating the disturbed development of conventional T cells, whereas the number of spleen cells and liver mononuclear cells was comparable to B6 mice (Fig. 2A). Among thymocytes, the number of CD4 single-positive (SP) thymocytes in Vα14/WTVβ mice was 30% that of B6 mice and was only 4% of normal in Vα14/Vβ7 mice, whereas the number of CD8 SP thymocytes was similar to B6 in both Vα14/WTVβ and Vα14/Vβ7 mice (Fig. 2B and C). The absolute number of DP thymocytes was severely diminished to 10 and 3% of B6 in Vα14/WTVβ and Vα14/Vβ7 mice, respectively (Fig. 2C). These decreases were observed despite the fact that genes important for the generation of T cells by secondary rearrangement events, such as RAG (26), RORγt (27), the antiapoptotic factors Bcl-xL (28) and Bcl2 (29) (encoded by *Rag1*, *Rag2*, *Rorc*, *Bcl2l1*, and *Bcl2*, respectively), were highly expressed by DP thymocytes in both Vα14/WTVβ and Vα14/Vβ7 mice (Fig. 2D). To investigate the secondary TCRα chain rearrangement underlying the appearance of non-NKT cells in NKT-iPSC-derived mice, we sorted conventional αβT cells defined as the α-GalCer/

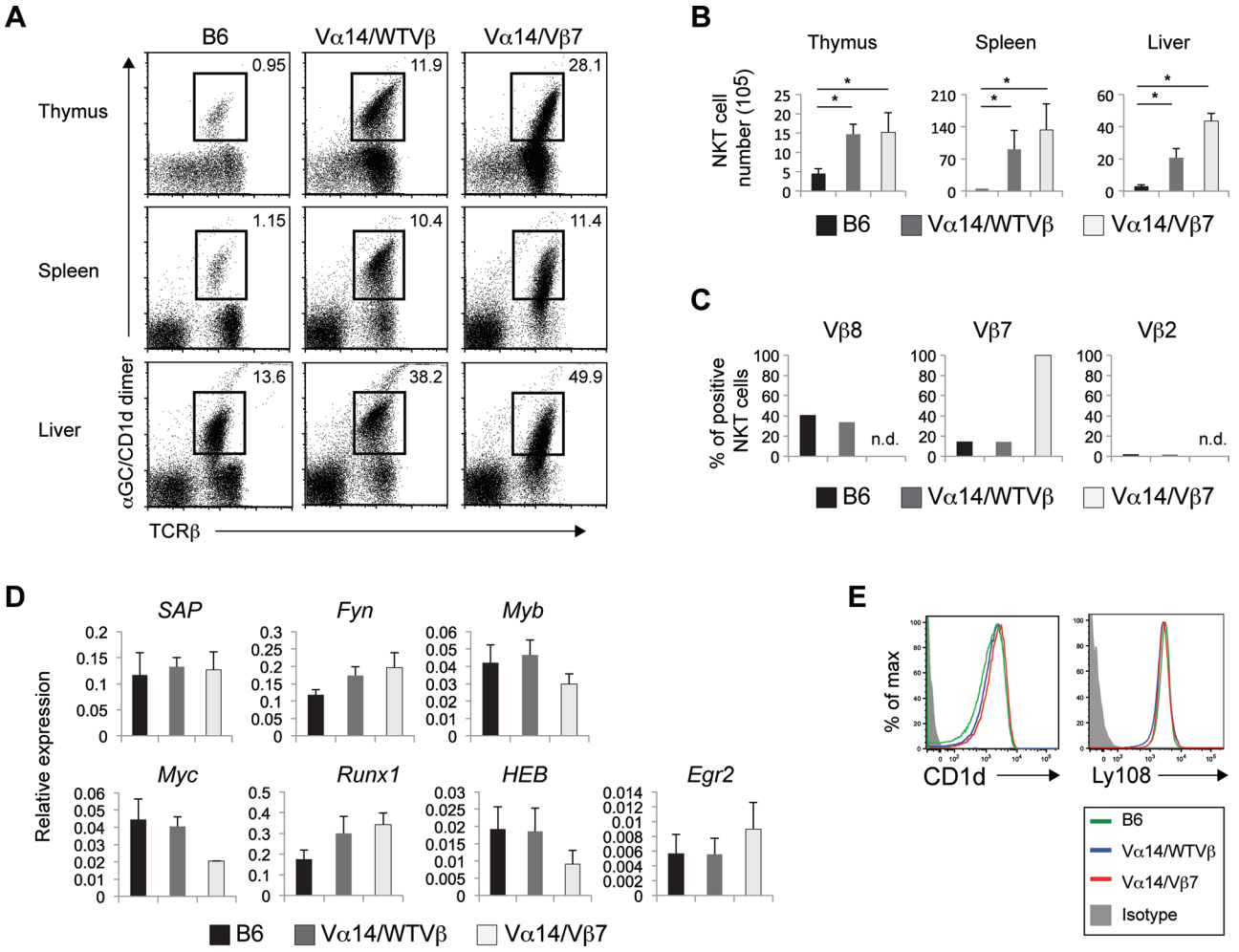

Fig. 1. Increase in the number of NKT cells in NKT-iPSC-derived mice. (**A** and **B**) Percentage (A) and absolute number (B) of NKT cells in the indicated organs of B6, Vα14/WTVβ and Vα14/Vβ7 mice. Data are presented as mean ± SD from three independent experiments. *$P < 0.01$ versus B6 group. (**C**) TCRVβ usage in splenic NKT cells of B6, Vα14/WTVβ and Vα14/Vβ7 mice. The frequency of Vβ-expressing cells within total α-GalCer/CD1d dimer$^+$ CD3ε$^+$ NKT cells is depicted. n.d., none detectable. (**D**) qPCR analysis of gene expression by FACS-sorted CD4/8 DP thymocytes from B6, Vα14/WTVβ and Vα14/Vβ7 mice. The data are normalized with *Gapdh* expression levels (mean ± SEM, $n = 3$). (**E**) CD1d and Ly108 expression by CD4/8 DP thymocytes from B6, Vα14/WTVβ and Vα14/Vβ7 mice. Representative FACS profiles of the gated CD4/8 DP thymocytes are shown. The open histograms indicate the staining with monoclonal antibodies. Each color represents the cells in the indicated organs. The grey histograms represent the isotype control.

CD1d$^-$ TCRβ$^+$ population shown in Fig. 1(A) from the thymus of Vα14/WTVβ mice and analyzed their TCRα chain usage by RT–PCR analysis. Results showed that these conventional αβ T cells expressed Trav6, 8D-1 and 10 located upstream of Vα14 (Trav11 according to the nomenclature by IMGT, the international ImMunoGeneTics information system, http://www.imgt.org) but did not express Trav1 and Trav2 (Supplementary Figure 2, available at *International Immunology* Online). As for the control, the Trav21, located downstream of Vα14, was not detected in these αβ T cells because the pre-rearranged Vα14Jα18 locus in Vα14/WTVβ mice should leave intact genome upstream of Vα14 (Trav11) and downstream of Jα18 (Traj18) but should have deletion of the genomic region downstream of Vα14 and upstream of Jα18. These data demonstrate that the α-GalCer/CD1d$^-$ but TCRβ$^+$ cells are conventional T cells that are derived by the secondary TCRα chain rearrangement events and furthermore suggest that conventional αβ T cells developed in NKT-iPSC-derived mice have limited TCRα chain repertoire.

The number of CD4/CD8 double-negative (DN) thymocytes was normal in Vα14/WTVβ mice, but was decreased to 40% of WT in Vα14/Vβ7 mice (Fig. 2C), indicating disturbed development as early as the thymic DN stage in Vα14/Vβ7 but not in Vα14/WTVβ mice. In order to investigate the development of DN thymocytes, we analyzed the DN stages of thymic ontogeny using CD117 and CD25 mAbs to distinguish the DN1 (CD117$^+$ CD25$^-$), DN2 (CD117$^+$ CD25$^+$), DN3 (CD117$^-$ CD25$^+$) and DN4 (CD117$^-$ CD25$^-$) stages. Results from flow cytometry analyses showed severely decreased DN3 stage thymocytes in heterozygous Vα14/Vβ7 mice while Vα14/WTVβ mice showed less dramatic changes although DN4 stage thymocytes were decreased compared with those from B6 mice (Supplementary Figure 3A and B, available at

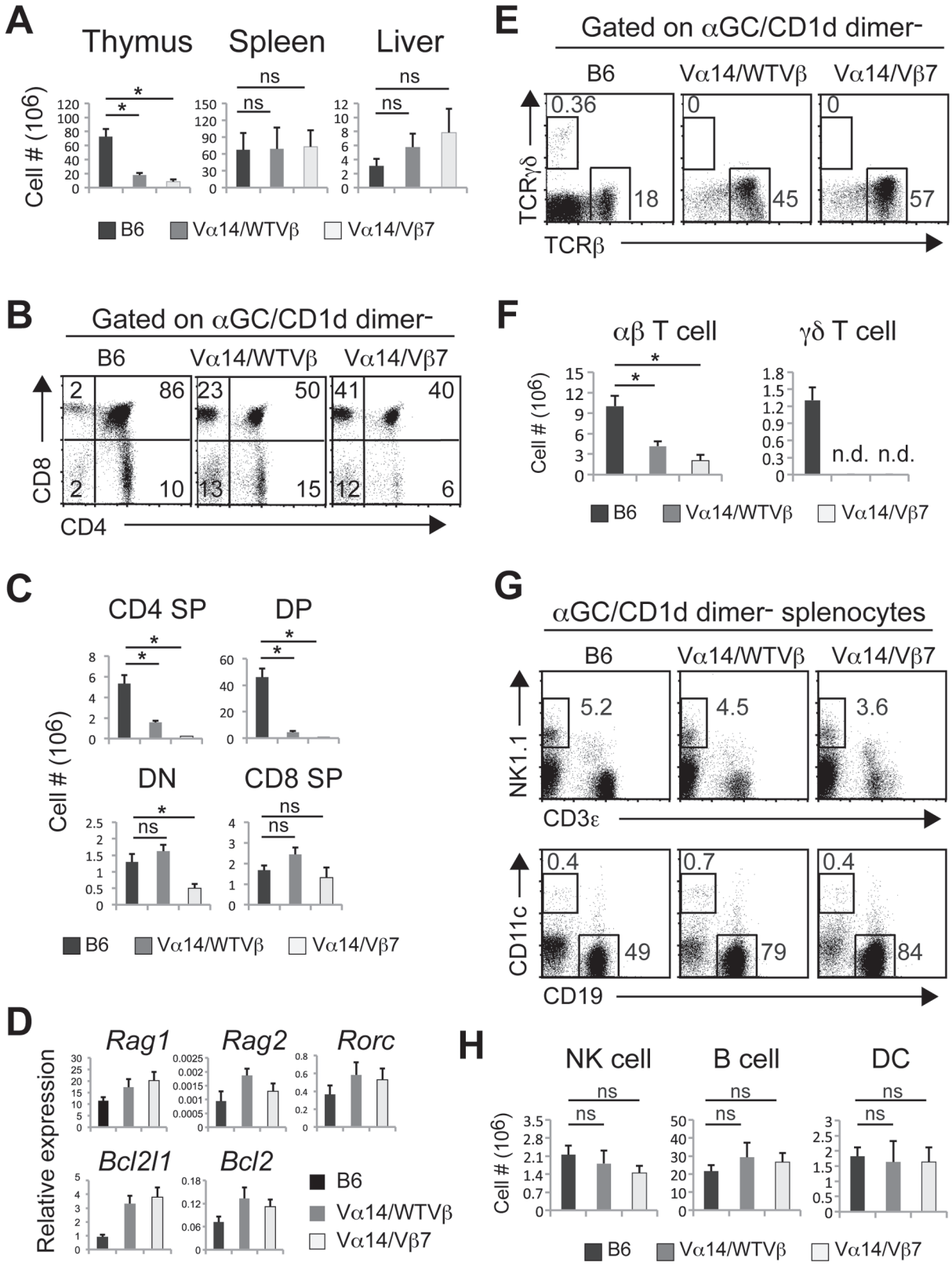

Fig. 2. Profiles of lymphocytes in NKT-iPSC-derived mice. (**A**) Absolute number of total mononuclear cells (MNCs) in the indicated organs of B6, Vα14/WTVβ and Vα14/Vβ7 mice. Data are presented as mean ± SD from three independent experiments. *$P < 0.01$ versus B6 group. ns, not statistically significant. (**B**) Representative FACS profiles of CD4/CD8 expression in α-GalCer/CD1d dimer negative thymocyte populations of B6, Vα14/WTVβ and Vα14/Vβ7 mice. (**C**) Absolute number of CD4 SP, CD4/8 DP, CD4/8 DN and CD8 SP cells in B6, Vα14/WTVβ and Vα14/Vβ7

International Immunology Online). These data suggest the pre-rearranged state of TCR genes in NKT-iPSC-derived mice causes the disturbed differentiation of DN thymocytes with more severe disturbances observed when both TCRα and TCRβ chains are pre-rearranged.

The frequency and cell number of other immune cells, such as αβT, γδT, NK, B and DCs in lymphoid organs of Vα14/WTVβ and Vα14/Vβ7 mice was also investigated. As shown in Fig. 2(E and F), no γδT cells were detected in the thymus of either Vα14/WTVβ or Vα14/Vβ7 mice, due to the loss of TCR δ locus by the Vα14Jα18 gene rearrangement events on both chromosomes (Supplementary Figure 1C, available at *International Immunology* Online). When the frequency and absolute number of splenic DC, B and NK cells was compared to that of B6 mice, no significant difference was observed in either Vα14/WTVβ or Vα14/Vβ7 mice (Fig. 2G and H).

We also analyzed T lymphocyte subsets in NKT-iPSC-derived mice, such as FOXP3$^+$ Treg cells and intraepithelial CD8αα T lymphocytes. Flow cytometry analyses revealed that both Treg and CD8αα cells are detected in Vα14/WTVβ and heterozygous Vα14/Vβ7 mice (Supplementary Figure 4A and B, available at *International Immunology* Online).

Taken together, these data suggest that both Vα14/WTVβ and Vα14/Vβ7 mice had preferential development of NKT cells and also grossly normal development of all immune cell types except for the absence of γδT and disturbed development of conventional CD4 αβT lymphocyte compartments, likely due to the pre-rearrangement of *Vα14Jα18* gene loci.

Development of NKT cell subtypes in Vα14/WTVβ and Vα14/Vβ7 mice

It has been shown that IL-17 receptor B (IL-17RB) and CD4 are reliable and distinct surface markers to distinguish IL-4-producing (CD4$^+$ IL-17RB$^+$), IL-17A-producing (CD4$^-$ IL-17RB$^+$) and IFN-γ-producing (IL-17RB$^-$) NKT cells (3). Therefore, the expression of CD4 and IL-17RB was investigated to define the frequency and absolute number of NKT cell subtypes in various tissues of the NKT-iPSC-derived mice.

The absolute number of all NKT cell subsets was increased about 3.2-fold in the thymus, 12.2-fold in the spleen and 9.0-fold in the liver of Vα14/WTVβ compared to B6 mice (Fig. 3A and B). Similarly, in Vα14/Vβ7 mice, the frequency and total NKT cell numbers were increased 3.4-fold in the thymus, 23.6-fold in the spleen and 18.4-fold in the liver, indicating a significant increase in all subsets of functional NKT cells in NKT-iPSC-derived mice. The frequency of NKT cell subsets was variable in the thymus of NKT-iPSC-derived mice but became relatively normal in the periphery.

Among the three functionally different NKT cell subsets, the CD4$^-$ IL-17RB$^+$ IL-17A-producing subset was dramatically increased in the Vα14/WTVβ and Vα14/Vβ7 mice (Fig. 3B and C). The increase was 45-fold in the thymus, 98-fold in the spleen and 73-fold in the liver of Vα14/WTVβ mice, and in Vα14/Vβ7 mice was 22-fold in the thymus, 57-fold in the spleen and 55-fold in the liver, compared to B6 mice.

There were also increases in the CD4$^+$ IL-17RB$^+$ NKT cells, which are characterized by IL-4 production. There was a 5- to 20-fold increase in their absolute number; in Vα14/WTVβ mice, their increases were 14- to 15-fold in all tissues, while in Vα14/Vβ7 mice, the fold increase was 5-fold in the thymus, 21 in the spleen and 16 in the liver, compared to B6 mice (Fig. 3B and C).

On the other hand, the IFN-γ-producing IL-17RB$^-$ NKT cells were increased only 2-fold in the thymus in Vα14/WTVβ mice and 3-fold in Vα14/Vβ7 mice, but were significantly increased in the peripheral tissues, 10-fold in the spleen and 8-fold in the liver of Vα14/WTVβ mice, and 24- and 18-fold in the spleen and liver in the Vα14/Vβ7 mice, compared to those of B6 mice (Fig. 3B and C).

Functional properties of NKT cell subtypes in Vα14/WTVβ and Vα14/Vβ7 mice

To investigate functional properties of the NKT cell subtypes in NKT-iPSC-derived mice, cytokine profiles were analyzed by intracellular staining to detect IFN-γ-, IL-4- and IL-17A- expressing NKT cells after activation with phorbol 12-myristate 13-acetate and ionomycin *in vitro* (Fig. 4A and B). The frequency and number of functional NKT cells in Vα14/WTVβ mice were increased 3.6-fold in the thymus, 8-fold in the spleen and 4.7-fold in the liver compared to B6 mice (Fig. 4A–C). Among these, the fold increases were 2.1 for IL-17A-producing NKT cells, 5.1 for the IL-4-producing NKT cells, and 2.8 for the IFN-γ-producing NKT cells, suggesting that there was no impairment in the normal development of functional NKT cells in Vα14/WTVβ mice (Fig. 4D).

On the other hand, in the thymus of Vα14/Vβ7 mice, total numbers of functional NKT cells were decreased by 20% compared to B6 mice, which is significantly lower than that in Vα14/WTVβ mice, where there was a 3.6-fold increase (Fig. 4C). Among the functional NKT cell subsets in the thymus of Vα14/Vβ7 mice, the IL-17A-producing and IL-4-producing NKT cells were 24 and 44%, respectively, of those in B6 mice, whereas the IFN-γ-producing NKT cells were increased 1.1-fold (Fig. 4D), demonstrating the significant developmental arrest in the thymus of Vα14/Vβ7 mice. Interestingly, however, in the peripheral tissues of these mice (Fig. 4C), there were global increases in total numbers of functional NKT cells (28.3-fold increase in the spleen, 5.6-fold in the liver) as well as in numbers of NKT subset cells (2.2-fold increase in IL-17A-producing NKT cells, 10 times in IL-4-producing NKT cells and 44-fold in IFN-γ-producing NKT cells in the spleen and 1.6-fold for IL-17A- and IL-4-producing NKT cells and 7.3-fold for IFN-γ-producing NKT cells in the liver) (Fig. 4D),

thymocytes. Data are presented as mean ± SD from three independent experiments. *$P < 0.01$ versus B6 group. ns, not statistically significant. (**D**) qPCR analysis of gene expression by FACS-sorted CD4/8 DP thymocytes of B6, Vα14/WTVβ and Vα14/Vβ7 mice. The data are normalized with *Gapdh* expression levels (mean ± SEM, $n = 3$). (**E** and **F**) Percentage (E) and absolute number (F) of αβ and γδ T cells in B6, Vα14/WTVβ and Vα14/Vβ7 thymocytes. Data are presented as mean ± SD from three independent experiments. *$P < 0.01$ versus B6 group. n.d., none detectable. (**G** and **H)** Percentage (G) and absolute number (H) of NK cells, B cells and DC in B6 Vα14/WTVβ and Vα14/Vβ7 splenocytes. Data are presented as mean ± SD from three independent experiments. *$P < 0.01$ versus B6 group. ns, not statistically significant.

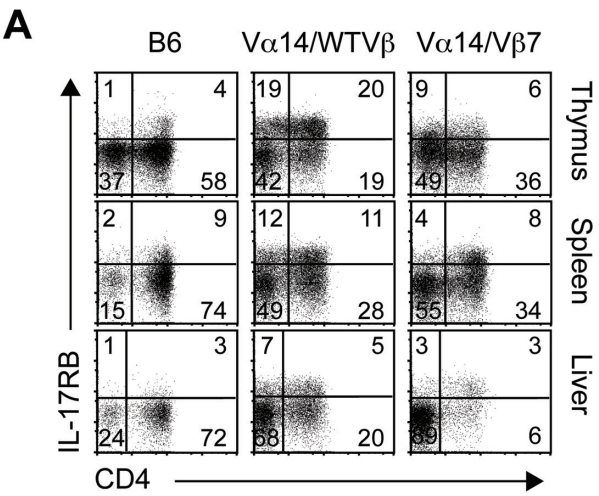

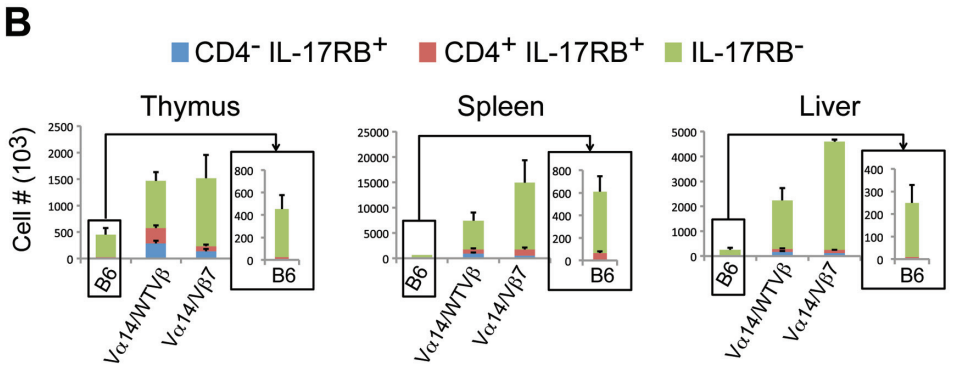

	Thymus			Spleen			Liver		
Cell number (×10³)	B6	Vα14/ WTVβ	Vα14/ Vβ7	B6	Vα14/ WTVβ	Vα14/ Vβ7	B6	Vα14/ WTVβ	Vα14/ Vβ7
CD4- IL-17RB+	6.3	284.7	136.5	9.2	899.0	522.3	2.2	163.5	123.9
CD4+ IL-17RB+	19.9	290.6	95.6	57.3	824.7	1208.7	7.7	118.7	123.9
IL-17RB-	426.3	892.2	1284.7	543.5	5698.8	13176.6	239.7	1957.8	4342.1
Total (Fold change)	452.5 (1)	1467.5 (3.2)	1516.8 (3.4)	610 (1)	7422.5 (12.2)	14408 (23.6)	249.6 (1)	2240 (9)	4589.9 (18.4)

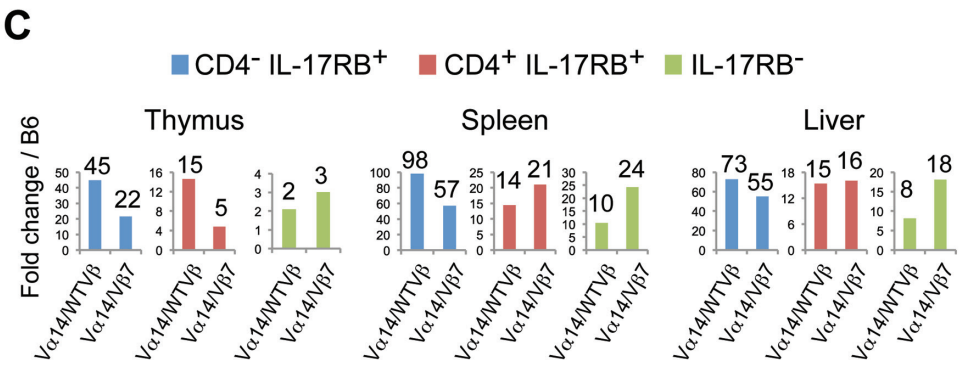

Fig. 3. NKT cell subsets in NKT-iPSC-derived mice analyzed by cell surface markers. (**A**) Representative FACS profiles of CD4/IL-17RB expression on the gated α-GalCer/CD1d dimer⁺ TCRβ⁺ NKT cell population in the indicated organs of B6, Vα14/WTVβ and Vα14/Vβ7 mice. (**B**) Absolute cell number of CD4⁻ IL-17RB⁺ (blue), CD4⁺ IL-17RB⁺ (red) and IL-17RB⁻ (green) fractions of NKT cells in the indicated organs from B6, Vα14/WTVβ and Vα14/Vβ7 mice. Actual absolute cell numbers are shown in the tables below the figures. Data are presented as mean ± SD from three independent experiments. (**C**) Fold changes in the number of cells in the different subsets of NKT cells over those of B6 mice are shown.

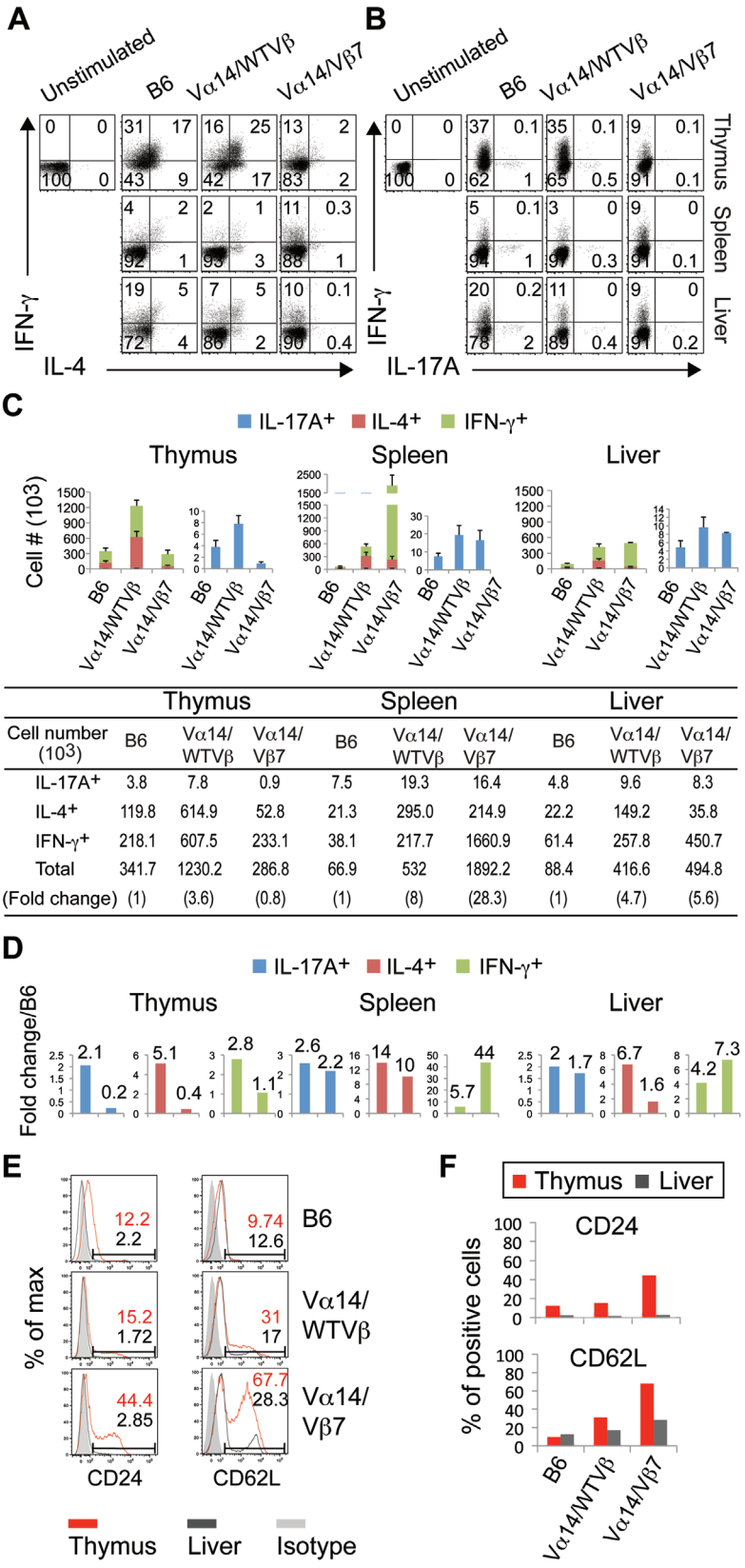

	Thymus			Spleen			Liver		
Cell number (10^3)	B6	Vα14/ WTVβ	Vα14/ Vβ7	B6	Vα14/ WTVβ	Vα14/ Vβ7	B6	Vα14/ WTVβ	Vα14/ Vβ7
IL-17A+	3.8	7.8	0.9	7.5	19.3	16.4	4.8	9.6	8.3
IL-4+	119.8	614.9	52.8	21.3	295.0	214.9	22.2	149.2	35.8
IFN-γ+	218.1	607.5	233.1	38.1	217.7	1660.9	61.4	257.8	450.7
Total	341.7	1230.2	286.8	66.9	532	1892.2	88.4	416.6	494.8
(Fold change)	(1)	(3.6)	(0.8)	(1)	(8)	(28.3)	(1)	(4.7)	(5.6)

Fig. 4. Functional NKT cell subsets in NKT-iPSC-derived mice analyzed by intracellular staining. (**A** and **B**) Intracellular staining for IFN-γ, IL-4 and IL-17A. NKT cells from the indicated organs were sorted and stimulated with Cell Stimulation Cocktail (plus protein transport inhibitors) for 4 h. Negative controls were nonstimulated B6 thymic NKT cells. Representative FACS profiles of IFN-γ/IL-4 and IFN-γ/IL-17A expression

indicating that the developmental arrest occurring in the thymus of Vα14/Vβ7 mice could be recovered in the peripheral tissues.

In agreement with the above findings shown in Fig. 4 (A–D), expression levels of CD24 (30) and CD62L (31), markers for the immature stage, were lower in liver NKT cells of Vα14/Vβ7 mice, while thymic NKT cells appeared immature based on their expression of high levels of CD24 and CD62L in comparison to Vα14/WTVβ and B6 mice (Fig. 4E and F). These data suggested that thymic NKT cells of Vα14/Vβ7 mice are rather immature but can mature in the peripheral tissues.

Discussion

Here, we have shown the successful generation of mice from NKT-iPSC made by reprogramming mature NKT cells of WT B6 mice. The two lines of NKT-iPSC-derived mice (Vα14/WTVβ and Vα14/Vβ7) both preferentially generate large numbers of NKT cells (Fig. 1A and B), a result consistent with previous reports showing that a preponderance of NKT cells resulted from introduction of the rearranged Vα14Jα18, either by a transgenic mouse approach (32) or by cloning mice from NKT-ES cells (NT-ESC) established by direct transfer of NKT cell nuclei into unfertilized eggs (33–35). The preferential development of NKT cells in NKT-iPSC-derived mice recapitulates results of *in vitro* experiments (7), indicating that the pre-rearranged Vα14 gene loci in the natural chromosomal context predispose developing thymocytes to an NKT cell fate. Alternatively, this outcome may be interpreted as being the result of higher proliferative responses of Vβ7-expressing NKT cells upon interaction with naturally expressed endogenous ligands (12).

Different from the preferential development of NKT cells, the number of total thymocytes other than NKT cells was strikingly decreased in both Vα14/WTVβ and Vα14/Vβ7 mice because of the severe reduction of conventional CD4 T cells associated with decreased numbers of DP cells and perturbed differentiation of DN stage thymocytes, which may be due to the existence of pre-rearranged TCRα loci on both alleles in the NKT-iPSC-derived mice and is reminiscent of results with TCR transgenic models (36, 37). By contrast, CD8 T-cell development was normal in the NKT-iPSC-derived mice, and one possible mechanism is that there exists a bypass mechanism, as proposed by Park *et al*. using MHC Class I-null mice (38). According to this model, the cytotoxic CD8 T-cell developmental pathway is not dependent *per se* on positive selection mechanisms with cognate MHC. Instead, signals emanating from the IL-7R can bypass TCR-MHC selection, resulting in the differentiation of CD8 T cells in the thymus. In addition, the limited TCR repertoire observed in T cells from NKT-iPSC-derived mice might result in the skewed development of CD8 T cells over CD4 T cells.

The most significant difference between the NKT-iPSC-derived mice and the previous *in vitro* studies using the NKT-iPSC was in the development of other immune cell lineages. In the *in vitro* studies, only NKT cells and a few macrophages, but no conventional T, B or DCs, could be generated from the NKT-iPSC line in either the OP9 or OP9/Dll1 culture system (7). However, the NKT-iPSC-derived mice, although they had disturbed development of conventional CD4 αβT lymphocytes, could generate all types of immune cells, except for γδ T cells (Fig. 2E and G), which was due to the elimination of TCRδ loci during the pre-rearrangement of Vα14 and Jα18 gene segments (see Supplementary Figure 1C, available at *International Immunology* Online). In addition, the NKT-iPSC-derived mice were fully pluripotent by virtue of their normal fertility and ability to reproduce progeny.

Thus, the NKT-iPSC-derived mouse appears to be a better model for NKT cell development and function study over transgenic mouse models, as abnormal development of immune cell types presented in transgenic mouse models (32, 39), as well as other problems might be caused by random integration of artificial promoters or unknown influences by the near-by genes in the integrated chromosome. Moreover, the large number of functional peripheral NKT cells residing in NKT-iPSC-derived mouse might represent another advantageous point for experiments involving cell transfer and measuring levels of molecules.

The number and frequency of the three subsets of NKT cells, $CD4^-$ IL-17RB$^+$, $CD4^+$ IL-17RB$^+$ and IL-17RB$^-$ NKT cells corresponding to IL-17A-, IL-4- and IFN-γ-producing NKT cell subsets, respectively, are all increased in both Vα14/WTVβ and Vα14/Vβ7 mice (Fig. 3A–C). However, the functional maturation of NKT cells was different among these NKT-iPSC-derived mice. In fact, the number and frequency of all functional NKT cell subsets in the Vα14/WTVβ mice are high in all tissues, and they are functionally mature in terms of their production of IL-17A, IL-4 and IFN-γ cytokines, while those in Vα14/Vβ7 mice, particularly the IL-17A- and IL-4-producing NKT cell subsets, are significantly lower in the thymus but increased in spleen and liver (Fig. 4A–D). These results suggest that NKT cells in Vα14/Vβ7 mice undergo functional maturation in the periphery. Consistently, thymic NKT cells from Vα14/Vβ7 mice are phenotypically immature based on higher expression levels of CD24 and CD62L, markers of very immature NKT cells (30) and naive conventional T cells (31), whereas these markers are downregulated in the peripheral NKT cells in Vα14/Vβ7 mice (Fig. 4E and F).

The immature state of thymic NKT cells from Vα14/Vβ7 mice might be related with their abnormally rapid development in the thymus, possibly induced by the pre-rearranged TCRβ loci in the chromosome. In agreement with this notion, the decreased number of DN thymocytes with severely diminished DN3 stage thymocytes observed in Vα14/Vβ7 mice (Fig. 2C and Supplementary Figure 3, available at

of the gated α-GalCer/CD1d dimer$^+$ TCRβ$^+$ NKT cells. (**C**) Absolute cell number of IFN-γ-producing (green), IL-4-producing (red) and IL-17A-producing (blue) NKT cells in thymus, spleen and liver of B6, Vα14/WTVβ and Vα14/Vβ7 mice. Data are presented as mean ± SD from three independent experiments. (**D**) Fold changes in the cell numbers of subsets of NKT cells compared to B6 mice are shown. (**E**) Representative FACS profiles of CD24 (left) and CD62L (right) expression by gated α-GalCer/CD1d dimer$^+$ TCRβ$^+$ NKT cells. The open histograms indicate staining with monoclonal antibodies. Each color represents the cells of the indicated organs. The grey histograms indicate the isotype control. (**F**) Percentage of CD24 (left) and CD62L (right) positive NKT cells in the indicated organs of B6, Vα14/WTVβ and Vα14/Vβ7 mice.

International Immunology Online) indicates the possibility of DN development stage skipping, due to the TCRβ pre-rearrangement, similar to a mouse model with a pre-rearranged TCRβ in a previous study (8).

It is important to compare the quality and function of the *in vitro* differentiated NKT cells with the *in vivo* differentiated NKT cells as the *in vitro* system using iPSC holds a potential to generate unlimited numbers of IFN-γ-producing functional NKT cells. Moreover, these *in vitro* differentiated NKT cells demonstrated promising characteristics of NKT cells when transferred into recipient mice by inducing adjuvant activity, which resulted in the augmented development of antigen-specific CD8 cytotoxic T cells and the bystander-activation of NK cells *in vivo*, although their surface phenotypes detected *in vitro* was reminiscent of immature NKT cells based on their high expression of CD24, double-positivity for CD4, CD8 expression etc. (7). In contrast to the *in vitro* differentiated NKT cells, the full functional maturation of NKT cells occurs in the peripheral organs, such as spleen and liver. Another noticed difference between the *in vitro* and the *in vivo* differentiated NKT cells is that the *in vitro* differentiated NKT cannot produce IL-17 (data not shown), while the *in vivo* differentiated NKT cells do produce IL-17 as shown in the present study. Therefore, it is tempting to conclude that the *in vitro* differentiated NKT cells are rather immature but would be functionally matured upon delivery to the tissue specific microenvironments *in vivo*.

Finally, it seems that the Vα14/WTVβ NKT-iPSC-derived mice described here and NKT clone mice with the rearranged Vα14Jα18 and germline Vβ generated by NT-ESC (34) are similar in terms of increased number of NKT cells even though they have an abnormality in thymocyte development. However, we demonstrate here that NKT cells from the NKT-iPSC-derived mouse show functional maturation in the peripheral organs by employing systematic analyses of surface phenotypes, gene expression and functional properties of NKT cells from the thymus, spleen and liver, which were not reported by Wakao *et al*. (34). It is also important to note that the main advantage of iPSC technology over the NT-ESC method is relatively convenience and ethical acceptability, because the iPSC technology does not require human oocytes for the generation of unlimited numbers of functional NKT cells with potential for clinical applications.

Funding

Grant-in-Aid for Scientific Research from the Ministry of Education, Culture, Sports, Science and Technology, Japan (24790490 to N.D., 23229005 and in part J2013606 to M.T.).

Acknowledgements

We thank Professor Peter Burrows, University of Alabama at Birmingham, for reading and editing of this manuscript. The authors also thank A. Ishige, T. Shigeura, R. Ozawa, M. Aihara, S. Sakata and Y. Nagata for excellent technical support and N. Takeuchi for secretarial assistance.

References

1 Taniguchi, M., Harada, M., Kojo, S., Nakayama, T. and Wakao, H. 2003. The regulatory role of Valpha14 NKT cells in innate and acquired immune response. *Annu. Rev. Immunol.* 21:483.
2 Bendelac, A., Savage, P. B., Teyton, L. 2007. The biology of NKT cells. *Annu. Rev. Immunol.* 25:297.
3 Watarai, H., Sekine-Kondo, E., Shigeura, T. *et al.* 2012. Development and function of invariant natural killer T cells producing T(h)2- and T(h)17-cytokines. *PLoS Biol.* 10:e1001255.
4 Nichols, K. E., Hom, J., Gong, S. Y. *et al.* 2005. Regulation of NKT cell development by SAP, the protein defective in XLP. *Nat. Med.* 11:340.
5 Kawakami, K., Yamamoto, N., Kinjo, Y. *et al.* 2003. Critical role of Valpha14$^+$ natural killer T cells in the innate phase of host protection against *Streptococcus pneumoniae* infection. *Eur. J. Immunol.* 33:3322.
6 Kawano, T., Cui, J., Koezuka, Y. *et al.* 1997. CD1d-restricted and TCR-mediated activation of valpha14 NKT cells by glycosylceramides. *Science* 278:1626.
7 Watarai, H., Fujii, S., Yamada, D. *et al.* 2010. Murine induced pluripotent stem cells can be derived from and differentiate into natural killer T cells. *J. Clin. Invest.* 120:2610.
8 Serwold, T., Hochedlinger, K., Inlay, M. A., Jaenisch, R. and Weissman, I. L. 2007. Early TCR expression and aberrant T cell development in mice with endogenous prerearranged T cell receptor genes. *J. Immunol.* 179:928.
9 Takahashi, K. and Yamanaka, S. 2006. Induction of pluripotent stem cells from mouse embryonic and adult fibroblast cultures by defined factors. *Cell* 126:663.
10 Terashima, A., Watarai, H., Inoue, S. *et al.* 2008. A novel subset of mouse NKT cells bearing the IL-17 receptor B responds to IL-25 and contributes to airway hyperreactivity. *J. Exp. Med.* 205:2727.
11 Watarai, H., Nakagawa, R., Omori-Miyake, M., Dashtsoodol, N. and Taniguchi, M. 2008. Methods for detection, isolation and culture of mouse and human invariant NKT cells. *Nat. Protoc.* 3:70.
12 Wei, D. G., Curran, S. A., Savage, P. B., Teyton, L. and Bendelac, A. 2006. Mechanisms imposing the Vbeta bias of Valpha14 natural killer T cells and consequences for microbial glycolipid recognition. *J. Exp. Med.* 203:1197.
13 Malissen, M., Trucy, J., Jouvin-Marche, E., Cazenave, P. A., Scollay, R. and Malissen, B. 1992. Regulation of TCR alpha and beta gene allelic exclusion during T-cell development. *Immunol. Today* 13:315.
14 Griewank, K., Borowski, C., Rietdijk, S. *et al.* 2007. Homotypic interactions mediated by Slamf1 and Slamf6 receptors control NKT cell lineage development. *Immunity* 27:751.
15 Pasquier, B., Yin, L., Fondanèche, M. C. *et al.* 2005. Defective NKT cell development in mice and humans lacking the adapter SAP, the X-linked lymphoproliferative syndrome gene product. *J. Exp. Med.* 201:695.
16 Chung, B., Aoukaty, A., Dutz, J., Terhorst, C. and Tan, R. 2005. Signaling lymphocytic activation molecule-associated protein controls NKT cell functions. *J. Immunol.* 174:3153.
17 Gadue, P., Morton, N. and Stein, P. L. 1999. The Src family tyrosine kinase Fyn regulates natural killer T cell development. *J. Exp. Med.* 190:1189.
18 Eberl, G., Lowin-Kropf, B. and MacDonald, H. R. 1999. Cutting edge: NKT cell development is selectively impaired in Fyn- deficient mice. *J. Immunol.* 163:4091.
19 Hu, T., Simmons, A., Yuan, J., Bender, T. P. and Alberola-Ila, J. 2010. The transcription factor c-Myb primes CD4$^+$CD8$^+$ immature thymocytes for selection into the iNKT lineage. *Nat. Immunol.* 11:435.
20 Dose, M., Sleckman, B. P., Han, J., Bredemeyer, A. L., Bendelac, A. and Gounari, F. 2009. Intrathymic proliferation wave essential for Valpha14$^+$ natural killer T cell development depends on c-Myc. *Proc. Natl Acad. Sci. USA* 106:8641.
21 Mycko, M. P., Ferrero, I., Wilson, A. *et al.* 2009. Selective requirement for c-Myc at an early stage of V(alpha)14i NKT cell development. *J. Immunol.* 182:4641.
22 Egawa, T., Eberl, G., Taniuchi, I. *et al.* 2005. Genetic evidence supporting selection of the Valpha14i NKT cell lineage from double-positive thymocyte precursors. *Immunity* 22:705.
23 D'Cruz, L. M., Knell, J., Fujimoto, J. K. and Goldrath, A. W. 2010. An essential role for the transcription factor HEB in thymocyte survival, Tcra rearrangement and the development of natural killer T cells. *Nat. Immunol.* 11:240.
24 Lazarevic, V., Zullo, A. J., Schweitzer, M. N. *et al.* 2009. The gene encoding early growth response 2, a target of the transcription

factor NFAT, is required for the development and maturation of natural killer T cells. *Nat. Immunol*. 10:306.
25 Gapin, L., Matsuda, J. L., Surh, C. D. and Kronenberg, M. 2001. NKT cells derive from double-positive thymocytes that are positively selected by CD1d. *Nat. Immunol*. 2:971.
26 Schlissel, M. S. 2003. Regulating antigen-receptor gene assembly. *Nat. Rev. Immunol*. 3:890.
27 Guo, J., Hawwari, A., Li, H. *et al.* 2002. Regulation of the TCRalpha repertoire by the survival window of CD4(+)CD8(+) thymocytes. *Nat. Immunol*. 3:469.
28 Ma, A., Pena, J. C., Chang, B. *et al.* 1995. Bclx regulates the survival of double-positive thymocytes. *Proc. Natl Acad. Sci. USA* 92:4763.
29 Linette, G. P., Grusby, M. J., Hedrick, S. M. *et al.* 1994. Bcl-2 is upregulated at the $CD4^+$ $CD8^+$ stage during positive selection and promotes thymocyte differentiation at several control points. *Immunity* 1:197.
30 Benlagha, K., Wei, D. G., Veiga, J., Teyton, L. and Bendelac, A. 2005. Characterization of the early stages of thymic NKT cell development. *J. Exp. Med*. 202:485.
31 Kovalovsky, D., Uche, O. U., Eladad, S. *et al.* 2008. The BTB-zinc finger transcriptional regulator PLZF controls the development of invariant natural killer T cell effector functions. *Nat. Immunol*. 9:1055.
32 Bendelac, A., Hunziker, R. D. and Lantz, O. 1996. Increased interleukin 4 and immunoglobulin E production in transgenic mice overexpressing NK1 T cells. *J. Exp. Med*. 184:1285.
33 Inoue, K., Wakao, H., Ogonuki, N. *et al.* 2005. Generation of cloned mice by direct nuclear transfer from natural killer T cells. *Curr. Biol*. 15:1114.
34 Wakao, H., Kawamoto, H., Sakata, S. *et al.* 2007. A novel mouse model for invariant NKT cell study. *J. Immunol*. 179:3888.
35 Watarai, H., Rybouchkin, A., Hongo, N. *et al.* 2010. Generation of functional NKT cells in vitro from embryonic stem cells bearing rearranged invariant Valpha14-Jalpha18 TCRalpha gene. *Blood* 115:230.
36 Lacorazza, H. D., Tucek-Szabo, C., Vasović, L. V., Remus, K. and Nikolich-Zugich, J. 2001. Premature TCR alpha beta expression and signaling in early thymocytes impair thymocyte expansion and partially block their development. *J. Immunol*. 166:3184.
37 Terrence, K., Pavlovich, C. P., Matechak, E. O. and Fowlkes, B. J. 2000. Premature expression of T cell receptor (TCR)alpha-beta suppresses TCRgammadelta gene rearrangement but permits development of gammadelta lineage T cells. *J. Exp. Med*. 192:537.
38 Park, J. H., Adoro, S., Guinter, T. *et al.* 2010. Signaling by intrathymic cytokines, not T cell antigen receptors, specifies CD8 lineage choice and promotes the differentiation of cytotoxic-lineage T cells. *Nat. Immunol*. 11:257.
39 Taniguchi, M., Koseki, H., Tokuhisa, T. *et al.* 1996. Essential requirement of an invariant V alpha 14 T cell antigen receptor expression in the development of natural killer T cells. *Proc. Natl Acad. Sci. USA* 93:11025.